DOI 10.1007/s11223-022-00376-5
Strength of Materials, Vol. 54, No. 1, January, 2022

ESTABLISHMENT OF STRESS CORROSION CRACKING QUANTITATIVE PREDICTION MODEL OF NICKEL-BASED ALLOY 600 AND ANALYSIS OF INFLUENCING FACTORS

Y. H. Cui[a], J. L. Zhang[b,c,1], and K. Zhao[c]

UDC 534.9

An important aspect of accurately predicting the stress corrosion cracking (SCC) growth rate of nuclear power welding joints and service materials is establishing the SCC growth rate prediction model, which is crucial for the safety assessment of nuclear power structural materials in autoclave environment and in-service residual life assessment. The SCC prediction model was analyzed and established based on creep-induced oxide film rupture. Results show that the SCC quantitative prediction model based on creep-induced oxide film rupture has good prediction accuracy. Through sensitivity analysis, which shows that the change of creep exponent n has the greatest influence on SCC growth rate, the sensitivity ranking of the other parameters from large to small is current decay exponent m and yield strength σ_y, rupture strain of oxide film ε_f, the oxidation current density i_0, time constant t_0 and power-law multiplier A, respectively.

Keywords: stress corrosion cracking, prediction model, nickel-based alloy 600, influence factor.

Introduction. Stress corrosion cracking (SCC) is a nuclear power structure's failure phenomenon under the combined action of stress, sensitive materials, and a corrosive environment. Another important research for predicting the crack growth rate (CGR) of nuclear power welding joints is establishing the SCC growth rate prediction model [1-2]. The research on SCC growth rate is also an important part of the safety assessment of nuclear power structure materials in an autoclave environment and the quantitative assessment of the remaining service life [3]. According to the experimental results of slip dissolution mechanism and fracture mechanics theory, scholars in this direction have proposed various prediction models to predict the SCC crack growth rate. Still, they have some limitations in characterizing the crack tip strain rate [4-7]. Nowadays, the general models for predicting SCC rate are divided into the following two types: one is the empirical prediction model of CGR based on many experiment results [8-9]. The second type is the deterministic prediction model of various parameters affecting the SCC growth rate, including the mechanical factors affecting the stress state around the crack zone and the electrochemical factors affecting the current density and the oxide film rupture. The CGR deterministic model must rely on the SCC mechanism. Experimental evidence shows that SCC is a complex process under the combined action of sensitive material, environment, and mechanics. A single mechanism can not explain the process of stress corrosion cracking [10]. The third type is the prediction model, which combines calculation, simulation, and SCC mechanism [11].

1. Establishment of the SCC Prediction Model of Nickel-Based Alloy 600.

Based on Faraday's law, the stress corrosion cracking of most nickel-based alloys and austenitic stainless steels can be explained by the slip dissolution mechanism of the anodic dissolution type under the autoclave environment [12].

[a]School of Mechanical & Electronic Engineering, Zhongyuan University of Technology, Zhengzhou 450007, China. [b]Xi'an Special Equipment Inspection Institute, Xi'an710065, China ([1]seii.zhangjl@qq.com). [c]School of Mechanical Engineering, Xi'an University of Science and Technology, Xi'an 710054, China. Translated from Problemy Mitsnosti, No. 1, p.8, January – February, 2022. Original article submitted March 8, 2021.

This is the famous Ford-Andresen prediction model. In this model, the oxide film rupture at the crack tip is measured by the limit strain of the crack tip strain rate reaching the passive film. Because this model can comprehensively reflect the influence of high-temperature water environment, material, and mechanical parameters at the crack tip on the CGR of the primary loop of the nuclear power plant. It has been widely recognized and applied in predicting SCC growth rate in high-temperature water environments. But, due to the complexity of the SCC crack tip service environment, it is hard to accurately obtain the only mechanical parameter crack tip strain rate in this model, making it difficult to accurately characterize the crack growth rate. Because the welded joint of nuclear power plants works for a long time under high temperatures, they bear larger stress around the crack zone, conforming to metal creep characteristics. The creep of alloy 600 and other materials under a high-temperature water environment has been confirmed by experiments. Hall also pointed out the leading role of creep in analyzing SCC crack tip strain rate under constant K [13]. Under constant *K* and *dK*/*da*, crack tip creep rate is the decisive parameter of SCC crack growth, which will lead to the increase of the crack tip stress and promotes creep and crack propagation.

$$\frac{da}{dt} = \frac{M}{\rho \cdot z \cdot F} \cdot \frac{i_0}{1-m} \left[\left(\frac{t_0 \cdot \dot{\varepsilon}_{ct}}{\varepsilon_f} \right)^m - m \cdot \left(\frac{t_0 \cdot \dot{\varepsilon}_{ct}}{\varepsilon_f} \right) \right] \tag{1}$$

Based on the fact that creep can occur and it also plays an important role in the SCC growth rate, our research team put forward the hypothesis that creep can lead to the oxide film rupture, and then the electrochemical reaction further leads to the SCC crack growth. And the key parameter crack tip creep is selected to replace the crack tip strain, as shown in Eq. (2):

$$\dot{\varepsilon}_{ct} = \dot{\varepsilon}_{cr} \tag{2}$$

where $\dot{\varepsilon}_{ct}$ and $\dot{\varepsilon}_{cr}$ represent the strain and creep at the crack tip, respectively.

Gary Was studied the creep characteristics of alloy 600 annealed at 337 and 360 ℃, which showed that the creep rate could be expressed via the relationship with experiment stress. Meanwhile, Wu and Sandstrom studied the low-alloy steel A508, which also shows that the relationship between the creep rate in the second stage and the test stress showed an exponential change, and the power-law model can also better express the constitutive creep law under high stress at the same time [14]. Therefore, the power-law model with an exponential relationship with stress can be expressed as Eq. (3) in the steady-state creep stage:

$$\dot{\varepsilon}_{cr} = A\sigma^n \tag{3}$$

where σ is the loading-induced stress, A and *n* are the constitutive creep parameters of materials.

Substituting Eq. (2) and Eq. (3) into Eq. (1), the prediction model of the SCC crack growth rate can be written as follows:

$$\begin{cases} \dot{a} = \dfrac{M}{\rho \cdot z \cdot F} \cdot \dfrac{i_0}{1-m} \left(\dfrac{t_0}{\varepsilon_f} \right)^m \left(\dot{\varepsilon}_{cr} \right)^m \\ \dot{\varepsilon}_{cr} = A\sigma^n \end{cases} \tag{4}$$

According to the creep power-law constitutive equation of the nickel-based alloy 600 at different temperatures, two prediction models of the SCC growth rate of this alloy at temperatures of 360 and 400 ℃ can be obtained, as follows:

$$\frac{da}{dt} = \frac{M}{Z \cdot \rho \cdot F} \times \frac{i_0}{1-m} \times \left(\frac{t_0}{\varepsilon_f} \right)^m \times \left(7.08 \times 10^{-16} \times \sigma^{3.77} \right)^m \tag{5}$$

$$\frac{da}{dt} = \frac{M}{Z \cdot \rho \cdot F} \times \frac{i_0}{1-m} \times \left(\frac{t_0}{\varepsilon_f} \right)^m \times \left(2.29 \times 10^{-16} \times \sigma^{4.02} \right)^m \tag{6}$$

As shown in (Eq. 5) and (Eq. 6), the oxide film will rupture due to the creep of base material at the crack tip, and the physical meaning of other parameters is explained in the F-A model.

2. Results and Discussions

2.1. Comparison of F-A, FRI, and Creep-Induced Film Rupture Models. By comparing the experimental results of the SCC growth rate in an autoclave environment, the rationality of the new SCC prediction model based on creep-induced film rupture can be evaluated. Considering the temperature in the nuclear power plant in actual service, the SCC growth rate prediction model of nickel-based alloy 600 at 360℃ is selected. The calculation of the SCC

growth rate requires parameters such as water chemical parameters and material mechanical properties. Among them, the current density of oxidation current at the crack tip of nickel-based alloy 600, time constant t_0, and the rupture strain of oxide film ε_f are measured in relevant literature [15], i_0 is between 0.01-0.02A/cm^2, t_0=0.4s, and m is between 0.4 and 0.42. Therefore, the hydrochemistry and material parameters of alloy 600 under a 360 ℃ water environment are shown in Table 1.

TABLE 1. Material parameters of nickel-based alloy 600 in the SCC environment

Electrochemical parameter	Value
Atomic weight, M (g/mol)	55.38
Charge change, Z	2.67
Oxidation current density, i_0 (A/mm^2)	0.001
Oxide film rupture strain, ε_f	0.001
Density, ρ (g/mm^3)	0.00786
Current decay curve exponent, m	0.4
Faraday constant, F (C/mol)	96500
Time constant, t_0 (s)	0.4

To verify the prediction accuracy of the creep-induced film rupture model, SCC growth rates under the three models are compared and analyzed. A comparison of prediction results is shown in Fig. 1. From Fig. 1, we can derive that the crack tip characteristic distance r_0 is an important parameter in the Ford-Andresen SCC life prediction model [7]. The prediction results of F-A and FRI models are closely related to the crack tip characteristic distance r_0. With the increase of characteristic distance r_0, the SCC rate decreases gradually. The gradient model of the crack tip is more sensitive to the feature distance when the feature distance r_0 is between 1 and 35 μm. The predicted value of the FRI model is about 2×10^{-9}~1×10^{-7}mm/s. The difference between the predicted values is nearly two orders of magnitude. The predicted value of the F-A model changes in 2×10^{-9}~2×10^{-6}m/s, the difference in predicted values is close to 3 orders of magnitude. Research shows that the F-A and FRI models have good prediction accuracy when the value of r_0 is between 2~10μm [16]. It also can be seen from Fig. 1 that when the characteristic distance r_0 at the crack tip is between 2 and 5 μm, the predicted SCC rate of the F-A model is 2×10^{-7}~8×10^{-7}mm/s, which is a little larger than that predicted by FRI model. The SCC growth rate predicted by the creep-induced film rupture model is 6×10^{-7}~8×10^{-7}mm/s. The CGR values predicted by the three models are basically in the same order of magnitude.

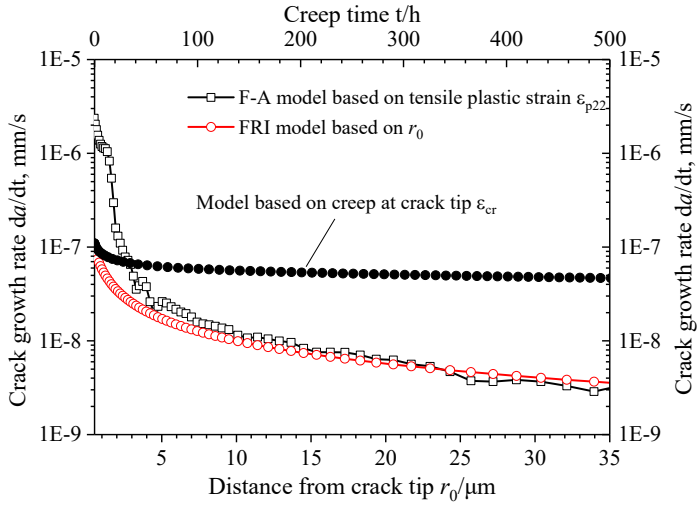

Fig. 1. Prediction results of different SCC quantitative prediction models for the nickel-based alloy 600

Based on the creep crack prediction model, the predicted SCC value is related to the creep time. Figure 1 shows that the SCC rate based on creep decreases with creep time. The variation range of the CGR-predicted value is about 2×10^{-9}~7×10^{-8}mm/s. According to the experimental analysis, the crack tip creep has reached a stable state after creeping for 200 h. Therefore, the creep rate obtained at this time can be used as the steady creep rate to predict CGR, and the CGR obtained can be used as the final predicted value. Therefore, we can conclude that the difference of

various creep rates obtained by the CGR prediction model based on creep is two-fold, which is less than 2.5 times of the FRI model, and far less than the difference of the F-A model at the crack tip. Within the variation range of characteristic distance and creep time shown in Fig. 1, the variation range of CGR-predicted value from small to large is the creep model, FRI model, and F-A model. The creep model is close to the prediction value of the FRI model, which shows that the newly established SCC quantitative prediction model based on crack tip creep has good prediction accuracy.

2.2. Comparison of SCC Prediction Model Based On Creep and SCC Experimental Data. Figure 2 shows the comparison between the nickel-based alloy 600 crack growth rate under different experimental conditions and the results of stress corrosion in the literature [17]. It can be seen that because there are many complex factors affecting SCC, the data have significant dispersion (there is a difference of several orders of magnitude under the same stress intensity factor K value). It is mainly caused by the composition of materials, processing heat treatment, environmental media, and other conditions [18]. For the samples with cold working in the T-L direction at 20% and 50%, the CGR doubled with the increased cold working degree. The SCC rate is about 5×10^{-8}~7×10^{-8}mm/s based on creep under the creep time t = 200 h. It can be seen from the comparison that the CGR value predicted by the proposed SCC rate prediction model based on crack tip creep and MRP-55 model under the same stress intensity factor K is only about three times different from that of SCC rate and experimental data under different experimental conditions.

Figure 3 shows the SCC experimental rates of nickel-based alloy 600 under different K obtained by Bettis laboratory under the primary water environment of nuclear power plants. From Fig. 3, one can see that the experimental data of crack growth rate are still very dispersive and also have a large difference rate under the same K. The creep rate at the crack tip in the SCC rate model based on creep is still calculated at t = 200 h. The new model predicts that the crack growth rate is about 5×10^{-8}~7×10^{-8}mm/s. It can be seen that with the increase of stress intensity factor K, the crack growth rate grows linearly. Through the comparative analysis of experimental data and model prediction results, it can be found that the SCC rate calculated by the SCC prediction model based on the new method is in the same order as the experimental data in the literature, and the rationality of the prediction model is further verified.

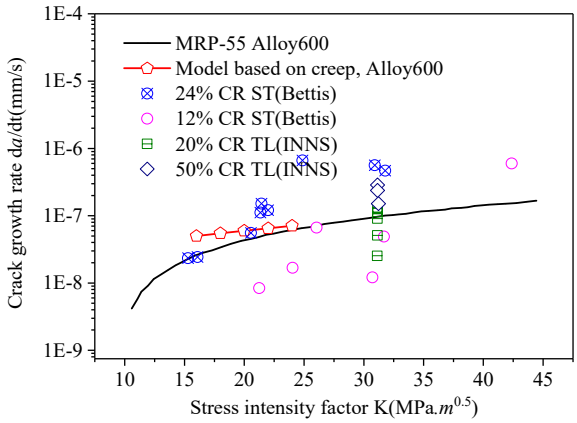

Fig. 2

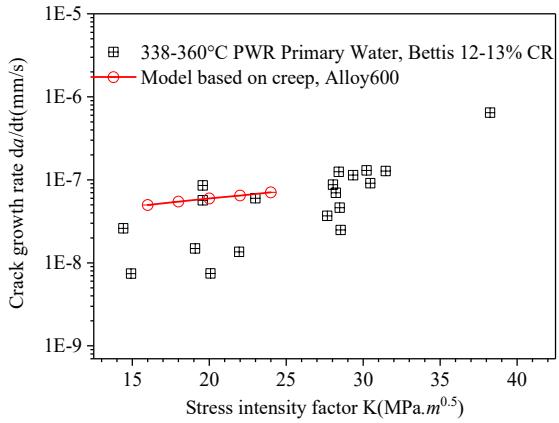

Fig. 3

Fig. 2. Predicted and experimental results obtained under different experimental conditions.
Fig. 3. Predicted and experimental results obtained at different stress intensity factors.

2.3. Analysis of Influencing Factors on SCC Rate. Through the analysis of the SCC prediction model based on creep, it can be seen that the main factors affecting the crack growth rate are mechanical and electrochemical factors, which mainly include K, A, n, crack tip stress σ, and the oxide film rupture strain ε_f. The electrochemical factors mainly include oxidation current density i_0, time constant t_0, and current decay curve exponent m.

To analyze the parameter sensitivity of the main influencing factors such as mechanics and electrochemistry, the influence rule of parameters in the uniform range on CGR is studied by normalizing the parameter range. Meanwhile, the sensitivity of the influencing factors is obtained by comparing the variation range of CGR in the same parameter range. Because the Young modulus of nuclear power structural materials has little change in the actual working conditions, it is not considered in the sensitivity analysis.

The parameters affecting the crack growth are set as abscissa, expressed as the proportional variation range of the four parameters. Based on the original basic data, the variation range is set as ±20%. The variation range of different materials, water chemistry, and load parameters of nickel-based alloy 600 is shown in Table 2.

TABLE 2. Variation ranges of electrochemical, material, and loading parameters of nickel-based alloy 600.

Electrochemical parameter	Value
Current decay curve exponent, m	0.32~0.48
Oxidation current density, i_0 (A/mm^2)	0.016~0.024
Stress intensity factor, $K(MPa{\cdot}m^{0.5})$	16~24
Oxide film rupture strain, ε_f	0.0008-0.0012
Time constant, t_0	0.32~0.48
Creep exponent, n	3.02~4.52
Stress at the crack tip, σ_y (MPa)	227~341
Time constant, t_0 (s)	0.32~0.48
Power-law multiplier, A	5.7×10^{-16}-8.5×10^{-16}

The effects of mechanical properties, crack tip load, and electrochemical parameters of the alloy 600 on the crack propagation rate are shown in Fig. 4, which shows that except for the current decay exponent m and oxide film rupture strain ε_f, the rest parameters are positively correlated with the crack growth rate. Thus, the SCC rate also shows an increasing trend with increased parameters. At the same time, the change in SCC rate caused by creep exponent is the largest under the same parameter variation ratio range, so creep exponent n has the greatest influence on the SCC rate, which is far greater than the influence of other factors and has the greatest sensitivity to the CGR.

To further compare the influence of relatively small sensitive parameters on CGR, the creep exponent n is removed. The sensitivity of the remaining material and electrochemical parameters to the growth rate is shown in Fig. 5. It also shows that the effects of power-law multiplier A, the oxide film current density i_0, the yield stres σ, and ε_f on the CGR are relatively weakl, and the sensitivity is relatively low within the same parameter variation range. The sensitivity of the power-law multiplier A is the lowest, and the other patterns are consistent with those in Fig. 4.

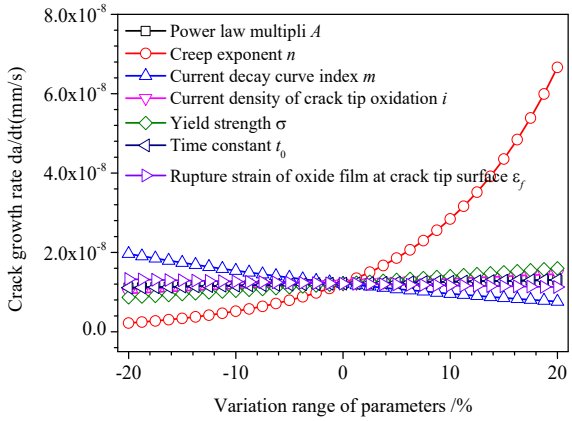

Fig. 4. Influence of the change of performance parameters of the nickel-based alloy 600 on CGR.

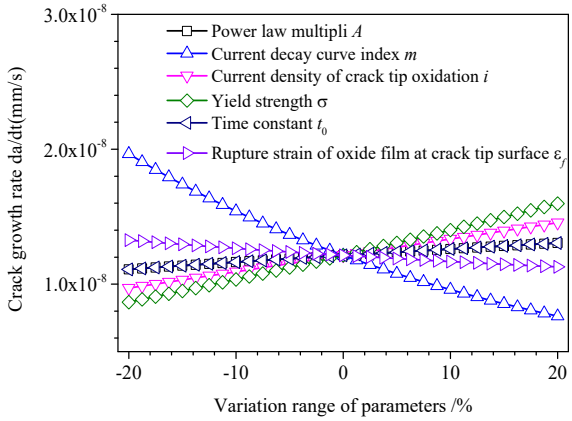

Fig. 5. Effects of other parameters on CGR, excluding the creep exponent n.

CONCLUSIONS

An SCC quantitative prediction model based on creep-induced oxide film rupture was established. Its comparison with the existing model and CGR experimental results proved its excellent prediction accuracy. Parameters m and ε_f negatively correlated with the SCC rate, while partameters σ_y, t_0, n, and i_0 positively correlated with the SCC rate. The sensitivity analysis revealed that the variation of n had the most significant effect on the SCC rate. The sensitivity ranking of other parameters in the decreasing order was as follows: m, σ_y, ε_f, i_0, t_0, and A.

Acknowledgment. This work was financially supported by the Natural Science Basic Research Plan in the Shaanxi Province of China (Grant No.2021JM-389) and Science and Technology Project of Shaanxi Market Supervision Administration (2021KY10).

REFERENCES

1. P. L. Andresen. "A brief history of environmental cracking in hot water," *Corrosion*, **75**, No. 3, 240-253 (2019).
2. Z. H. Li, Y. H. Lu, X. Y. Wang, "Modeling of stress corrosion cracking growth rates for key structural materials of nuclear power plant," *J. Mater. Sci.*, **55**, No. 2, 439-463 (2020).
3. J. L. Zhang, Y. H. Cui, H. Xue, et al., "Research on SCC Crack Growth Behavior of Nickel-based Alloy 600 in Safe-end Welded Joints," *Rare Metal Mat. Eng.,* **49**, No. 5, 1496-1502 (2020).
4. Z. P. Lu, T. Shoji, H. Xue, et al., "Deterministic formulation of the effect of stress intensity factor on PWSCC of Ni-base alloys and weld metals," *J. Press. Vess-T*, **135**, No. 2, (2013).
5. T. Shoji, S. Suzuki, R. G. Ballinger, "Theoretical prediction of SCC growth behavior--Threshold and plateau growth rate," *7th Int. Symp. on Environmental Degradation of Materials In Nuclear Power Systems--Water reactors: Proceedings and symposium discussions,* No. 2, (1995).
6. T. Shoji, Z. P. Lu, H. Xue, et al. "Quantification of the effects of crack tip plasticity on environmentally-assisted crack growth rates in LWR environments," *Environment-Induced Crack. Mater.*, No. **2**, 107-122 (2008).
7. H. Xue, Y. Sato, T. Shoji. "Quantitative estimation of the growth of environmentally assisted cracks at flaws in light water reactor components," *J. Press. Vess-T ASME*, **131**, No. 1, 61-70 (2009).
8. M. B. Toloczko, S. M. Bruemmer, "Crack growth response of alloy 690 in simulated PWR primary water," *14th Int. Conf. on Environmental Degradation of Materials in Nuclear Power Systems Water Reactors* 706-721 (2009).
9. P. L. Andresen, K. Gott, J. L. Nelson. "Stress corrosion cracking of sensitized type 304 stainless steel in 288C water: a five laboratory round robin," *9th Int. Symp. on Environmental Degradation of Materials in Nuclear Power Systems-Water Reactors*, John Wiley & Sons, Inc., 423-433 (1999).
10. F. P. Ford, "Quantitative prediction of environmentally assisted cracking," *Corrosion*, **52, No.** 5, 375-395 (1996).
11. J. Shi, J. Wang, D. D. Macdonald. "Prediction of primary water stress corrosion crack growth rates in Alloy 600 using artificial neural networks," *Corros. Sci.*, **92**, 217-227 (2015).
12. P. L. Andresen. "Environmentally assisted growth rate response of nonsensitized AISI 316 grade stainless steels in high temperature water," *Corrosion*, **44**, No. 7, 450-460 (1988).
13. M. M. Hall Jr, "Critique of the Ford-Andresen film rupture model for aqueous stress corrosion cracking," *Corros. Sci.*, **51**, No. 5, 1103-1106 (2009).
14. R. Wu, S. Sandfeld. "A dislocation dynamics-assisted phase field model for Nickel-based superalloys: The role of initial dislocation density and external stress during creep," *J. Alloy Compd.*, **703**, 389-395 (2017).
15. S. A. Attanasio, J. S. Fish, et al., "Measurement of the Fundamental Parameters for the Film in rupture/Oxidation Mechanism," *9th Int. Symp. on Environmental Degradation of Materials in Nuclear Power Systems* (1999).
16. Q. Peng, J. Kwon, T. Shoji, et al., "Development of a fundamental crack tip strain rate equation and its application to quantitative prediction of stress corrosion cracking of stainless steels in high temperature oxygenated water," *J. Nucl. Mater.*, **324**, No. 1, 52-61 (2004).
17. G. White, J. Hickling, L. Mathews, "Crack Growth Rates for Evaluating PWSCC of Thick–Wall Alloy 600 Material," *Proc. of the 11th Intl. Symp. on Environmental Degradation of Materials in Nuclear Power Systems-Water Reactors, NACE International, Houston, TX*, 166-179 (2003).
18. A.R. Jenks, G. A. White, P. Crooker, "Crack growth rates for evaluating PWSCC of thick-wall alloy 690 material and alloy 52, 152, and variant welds," *Proc. of ASME 2017 Pressure Vessels and Piping Conference* (2017).